



RESEARCH ARTICLE

Oxidative stress induces monocyte-to-myofibroblast transdifferentiation through p38 in pancreatic ductal adenocarcinoma

Xin Huang^{1,2,3}  | Chaobin He^{1,2,3} | Xin Hua^{1,2,4} | Anna Kan^{1,2,5} | Yize Mao^{1,2,3} | Shuxin Sun^{1,2,3} | Fangting Duan^{1,2,3} | Jun Wang^{1,2,3} | Peng Huang^{1,2} | Shengping Li^{1,2,3} 

¹State Key Laboratory of Oncology in South China, Collaborative Innovation Center for Cancer Medicine, Sun Yat-sen University Cancer Center, Guangzhou, People's Republic of China

²Department of Experimental Research, Sun Yat-sen University Cancer Center, Guangzhou, People's Republic of China

³Department of Pancreatobiliary Surgery, Sun Yat-sen University Cancer Center, Guangzhou, People's Republic of China

⁴Department of Medical Oncology, Sun Yat-sen University Cancer Center, Guangzhou, People's Republic of China

⁵Department of Hepatic Surgery, Sun Yat-sen University Cancer Center, Guangzhou, People's Republic of China

Correspondence

Shengping Li, State Key Laboratory of Oncology in South China, Collaborative Innovation Center for Cancer Medicine, Sun Yat-sen University Cancer Center, Guangzhou 510060, People's Republic of China.
Email: lishengp@mail.sysu.edu.cn

Funding information

National Natural Science Foundation of China, Grant/Award Number: 81672390; National Key Research and Development Plan, Grant/Award Number: 2017YFC0910002

Xin Huang, Chaobin He and Xin Hua contributed equally to this work.

Abstract

Background: Cancer-associated fibroblasts (CAFs) are among the most prominent cells during the desmoplastic reaction in pancreatic ductal adenocarcinoma (PDAC). However, CAFs are heterogeneous and the precise origins are not fully elucidated. This study aimed to explore whether monocytes can transdifferentiate into fibroblasts in PDAC and evaluate the clinical significance of this event.

Methods: CD14⁺ monocytes were freshly isolated from human peripheral blood. Immunofluorescence, reverse transcription-quantitative PCR, western blot, flow cytometry and enzyme-linked immunosorbent assay were used to detect the expression of α SMA, fibronectin, and other relevant molecules. In addition, latex beads with a mean particle size of 2.0 μ m were used to assess the phagocytic capacity. Moreover, RNA sequencing (RNA-seq) was performed to identify the differences induced by H₂O₂ and the underlying mechanisms.

Results: Immunofluorescence identified α SMA and fibroblast-specific protein 1 expression by tumor-associated macrophages in PDAC. The in vitro experiment revealed that oxidative stress (H₂O₂ or radiation) induced monocyte-to-myofibroblast

Abbreviations: CAFs, cancer-associated fibroblasts; CCK-8, cell counting kit-8; Col1, collagen1; DEGs, differentially expressed genes; DMSO, dimethyl sulfoxide; ECM, extracellular matrix; ELISA, enzyme-linked immunosorbent assay; FAP, fibroblast activation protein; FPKM, fragments per kilobase of exon per million fragments mapped; FSP1, fibroblast-specific protein 1; HMDMs, human monocyte-derived macrophages; iCAFs, inflammatory cancer-associated fibroblasts; IF, immunofluorescence; KEGG, Kyoto Encyclopedia of Genes and Genomes; MMT, monocyte-to-myofibroblast transdifferentiation; MSCs, mesenchymal stem cells; NFs, normal fibroblasts; PBMCs, peripheral blood mononuclear cells; PDAC, pancreatic ductal adenocarcinoma; PSCs, pancreatic stellate cells; ROS, reactive oxygen species; RT-qPCR, reverse transcription-quantitative polymerase chain reaction; TAMs, tumor-associated macrophages; WB, western blot; MAPK, mitogen-activated protein kinase.

This is an open access article under the terms of the Creative Commons Attribution License, which permits use, distribution and reproduction in any medium, provided the original work is properly cited.

© 2020 The Authors. *Clinical and Translational Medicine* published by John Wiley & Sons Australia, Ltd on behalf of Shanghai Institute of Clinical Bioinformatics

transdifferentiation (MMT), as identified by upregulated α SMA expression at both the RNA and protein levels. In addition, compared with freshly isolated monocytes, human monocyte-derived macrophages increased fibronectin expression. RNA-seq analysis identified p53 activation and other signatures accompanying this transdifferentiation; however, the p53 stabilizer nutlin-3 induced α SMA expression through reactive oxygen species generation but not through the p53 transcription/mitochondria-dependent pathway, whereas the p38 inhibitor SB203580 could partially inhibit α SMA expression. Finally, MMT produced a unique subset of CAFs with reduced phagocytic capacity that could promote the proliferation of pancreatic cancer cells.

Conclusions: Oxidative stress in the tumor microenvironment could induce MMT in PDAC, thus inducing reactive stroma, modulating immunosuppression, and promoting tumor progression. Reducing oxidative stress may be a promising future therapeutic regimen.

KEY WORDS

monocyte-to-myofibroblast transdifferentiation, oxidative stress, p38, p53, pancreatic ductal adenocarcinoma

1 | INTRODUCTION

Pancreatic ductal adenocarcinoma (PDAC) is a notoriously aggressive cancer with a 5-year survival rate of less than 10% and is projected to be the second leading cause of cancer deaths by 2030.^{1,2} Due to local invasion and distant metastasis, only 20% of patients are candidates for surgical resection, which remains the sole potentially curative option because of relative resistance to chemotherapy, radiotherapy, or immunotherapy.^{3,4}

PDAC is characterized by an extensive fibrotic response. The main components of the stroma are cancer-associated fibroblasts (CAFs), tumor-associated macrophages (TAMs), vascular endothelial cells, extracellular matrix (ECM), and so forth. CAFs are characterized by the expression of α SMA, fibroblast-specific protein 1 (FSP1), fibroblast activation protein (FAP), collagen1 (Col1), or fibronectin, and α SMA is the most classical and acceptable marker, which is also expressed by vascular smooth muscle cells and associated with cell contractility.⁵ CAFs in PDAC are thought to promote cancer initiation and progression, and to induce chemoresistance by secreting chemokines and ECM, which impedes the delivery of therapeutic agents.⁶ However, targeting CAFs leads to PDAC disease progression in both humans and mice.^{7,8} In addition, other researchers have reported that stromal elements act to suppress rather than support pancreatic cancer development.⁹ These studies highlighted the heterogeneity of CAFs, which might be ascribed to the numerous potential origins of CAFs.¹⁰ In other cancers, local proliferation of res-

ident fibroblasts, epithelial-to-mesenchymal transition, and endothelial-to-mesenchymal transition have been reported to contribute to the CAFs population.¹¹ In PDAC, quiescent pancreatic stellate cells (PSCs) and mesenchymal stem cells (MSCs) have been reported to contribute to the CAFs pool.^{12,13}

TAMs have an important role in promoting PDAC progression.¹⁴ Human blood monocytes are recruited into PDAC tissues, where they differentiate into macrophages. These human monocyte-derived macrophages (HMDMs) face an unfavorable environment characterized by accumulation of reactive oxygen species (ROS), which are generated as byproducts of intracellular oxygen metabolism or in response to exogenous stimuli, including chemotherapeutics and ionizing radiation. Generally, moderate levels of ROS act as signals to promote cell survival and function, whereas a severe increase in ROS levels can induce cell death.¹⁵ Studies have shown that ROS are essential for monocyte survival and differentiation.¹⁶ Other researchers used 200 μ M H₂O₂ to induce oxidative stress and found that ROS induced CCR5 expression by monocytes.¹⁷ Another study demonstrated that 100 μ M H₂O₂ stimulated monocytes/macrophages to actively release HMGB1.¹⁸ Recently, other reports have indicated that ROS induce PD-L1 expression by TAMs in breast cancer.¹⁹

Transdifferentiation is a process of lineage reprogramming whereby one terminally differentiated somatic cell directly transforms into another mature somatic cell.^{20,21} Tanabe et al recently reported that human adult peripheral blood T lymphocytes can be directly converted into fully functional

neurons.²² Other reports have indicated that pre-B cells,²³ smooth muscle cells,²⁴ and fibroblasts²⁵ can transdifferentiate into macrophages.

The density of macrophages correlates with that of α SMA⁺ fibroblasts and with Col1 deposition in PDAC.²⁶ Numerous studies have shown that macrophages are located very near myofibroblasts and could regulate fibrosis by producing profibrotic mediators, including TGF- β 1.^{27,28} In addition, other studies have reported that subsets of TAMs express FSP1, FAP, or Col1, which are relatively specific to fibroblasts.²⁹⁻³¹ Research on fibrotic diseases, such as renal fibrosis, has indicated that bone marrow-derived monocytes can transdifferentiate into myofibroblasts via a process termed monocyte-to-myofibroblast transdifferentiation (MMT).³² However, MMT has not been explored clearly in cancers, and its molecular mechanism has not been fully elucidated.

ROS have been reported to promote myofibroblast differentiation and tumor spreading in cancers.³³ In this study, we demonstrated for the first time that cellular oxidative stress can induce human monocytes to transdifferentiate into CAFs in PDAC, thus promoting fibrosis, hampering the immune reaction, and promoting tumor progression.

2 | METHODS

2.1 | Isolation and culture of cells

CD14⁺ monocytes were enriched from peripheral blood mononuclear cells (PBMCs) as previously described.³⁴ Monocytes were cultured in serum-free DMEM for 30 min in 5% CO₂ at 37°C in order to allow adhesion, and then cultured in DMEM containing 10% human AB serum (100-318; Gemini). Medium was collected or replaced every 3-4 days.

Human PDAC cell lines (AsPC-1, BxPC-3, CFPAC-1, and PANC-1) and HPDE6-C7 were cultured, and the cell supernatant was collected for 24 h.³⁴

PSCs were isolated as others,³⁵ including CAFs from tumor tissue and normal fibroblasts (NFs) from matching normal tissue of the same patient. Cell populations between passage 3 and 6 were used.

2.2 | Drugs treatment

Nutlin-3 was purchased from Selleck Chemicals (S1061; USA), dissolved in dimethyl sulfoxide (DMSO), and stored at -20°C. TGF- β 1 (100-21; Peprotech, USA) or H₂O₂ (323381; Sigma Aldrich) was added into the culture medium. Considering the rapid metabolism of H₂O₂, exogenous H₂O₂ was added twice a day. To inhibit p53 transcription or translocation activity, monocytes were pretreated with PFT- α (S5791; Selleck) or PFT- μ (S2930; Selleck), respectively. The p38 specific

Highlights

1. Myofibroblast-specific markers (α SMA and FSP1) were expressed by TAMs in pancreatic ductal adenocarcinoma.
2. Oxidative stress induced MMT in a time- and concentration-dependent manner by activating p38-MAPK pathway.
3. MMT defined a unique subset of CAFs with reduced phagocytic capacity.

inhibitor, SB203580 (S1076; Selleck), was added 30 min prior to the addition of other drugs. In addition, 100 U/mL catalase (C1345; Sigma Aldrich) was added daily to eradicate the intracellular H₂O₂.

2.3 | Radiation

Cells were irradiated (0, 2, 4, 8, or 16 Gy) as previously described.³⁶

2.4 | Cell viability

Cell viability was examined by a Cell Counting Kit-8 (CCK-8; Dojindo, Japan) assay to investigate an appropriate concentration of H₂O₂ or radiation dose for monocytes cultured in vitro. A total of 1.25×10^5 cells were plated into 96-well plates giving a final volume of 200 μ L of culture medium with 0, 50, 100, 200, 300, 500, or 1000 μ M H₂O₂; or cells were irradiated with 0, 2, 4, or 8 Gy. After incubation for the indicated time (1, 3, or 7 days), the cultured medium was removed; we added CCK-8 reagent (incubation at 37°C for 2 h) and measured the absorption at 450 nm (Bio-Rad Laboratories, USA).

The cell viability of cancer cells exposed to different treatments was detected as described above, with 2000-3000 cells plated into 96-well plates and cultured for the indicated time. For the supernatant, 2×10^5 monocytes were treated with 100 μ M H₂O₂ (twice a day) or not for 7 days in 6-well plates, and then the medium was changed to complete medium supplemented with 10% fetal bovine serum. Similar to other study,³⁷ after 36 h, supernatant was centrifuged and collected.

2.5 | Flow cytometry

Freshly isolated monocytes were stained with PE/Cy7-conjugated anti-CD14 (301814; Biolegend).³⁴ For ROS

measurement, monocytes were seeded at 0.5×10^6 cells/mL and treated with H_2O_2 , irradiation, nutlin-3, or DMSO. After the indicated time periods, cells were washed with PBS and resuspended with $10 \mu M$ H2DCFDA (D399; Invitrogen) in the dark for 30 min at $37^\circ C$. Cells were then washed for twice. Fluorescence was measured and data of mean fluorescence intensity were analyzed by Kaluza (Beckman Coulter, USA).

2.6 | Reverse transcription-quantitative polymerase chain reaction

Reverse transcription-quantitative polymerase chain reaction (RT-qPCR) was performed as described previously.³⁴ The primer sequences were listed in the Table S1.

2.7 | Western blot

We performed western blot (WB) analysis as previously described³⁶ using an ECL kit (4AW011; purchased from 4A Biotech Co., Ltd) and the following antibodies: anti-GAPDH (1:5000, 60004-1-Ig; Proteintech, USA), anti- α SMA (1:1000, ab124964; Abcam, UK), anti-fibronectin (1:1000, ab45688; Abcam, UK), anti-MDM2 (1:1000, #86934; Cell Signaling Technology, USA), anti-t-p53 (1:1000, 10442-1-AP; Proteintech, USA), anti-Col1 (1:1000, #84336; Cell Signaling Technology, USA), anti-vimentin (1:1000, #5741; Cell Signaling Technology, USA), anti-CD68 (1:5000, 25747-1-AP; Proteintech, USA), anti-p-p38 (1:1000, #4511; Cell Signaling Technology, USA), anti-t-p38 (1:1000, #8690; Cell Signaling Technology, USA), anti-p21 (1:1000, ab109520; Abcam, UK), and anti-FSP1 (1:1000, ab124805; Abcam, UK).

2.8 | Cell and tissue immunofluorescence

Cell or tissue immunofluorescence (IF) staining was performed as previously reported^{34,36}; cells were incubated with anti- α SMA (1:300), FSP1 (1:100), or anti-CD68 (1:100, ZM-0464; Zhongshan Golden Bridge Biotechnology Co., Beijing, China) overnight at $4^\circ C$.

2.9 | Enzyme-linked immunosorbent assay

Human fibronectin from cell culture supernatant was detected by enzyme-linked immunosorbent assay (ELISA) (CSB-E04551h; Cusabio Biotech, Houston, TX, USA); 96-well plates were read at 450 and 540 nm and data were analyzed as others.³⁸

2.10 | Phagocytosis of latex beads

Human monocytes were incubated with or without $100 \mu M$ H_2O_2 for the indicated time. Cells were starved for 12 h and incubated with latex beads (L3030; Sigma) with a mean particle size of $2.0 \mu m$ for 24 h; they were processed as aforementioned cell IF. When cells phagocytosed numerous latex beads, they became red in fluorescent microscope. Phagocytotic activity was calculated as the number of cells phagocytosing beads divided by the number of nuclei.²⁴

2.11 | RNA sequencing library preparation and transcriptomic analysis

Monocytes were cultured with or without $100 \mu M$ H_2O_2 for 7 days. Respective total RNAs were extracted and random primers were used to generate cDNA. Sequencing was carried out using an Illumina HiSeq 4000 Sequencing System for 150 cycles (KangChen Bio-tech Inc, Shanghai, China). After the data preprocessing, fragments per kilobase of exon per million fragments mapped (FPKM) and differentially expressed genes (DEGs) were then calculated,^{39,40} with the FPKM ≥ 0.5 (Cuffquant) considered statistically significant. Furthermore, Kyoto Encyclopedia of Genes and Genomes (KEGG) tool was used for pathway analysis of the DEGs.

2.12 | Statistical analysis

Data are expressed as the means \pm standard errors of the mean. We used independent or paired *t*-test or a Wilcoxon matched-pairs test for comparison between groups, and one-way or two-way ANOVA with the Bonferroni's post hoc test for multiple comparisons. GraphPad prism 7 was used for statistical analysis using two tailed tests and $P < .05$ was considered statistically significant.

3 | RESULTS

3.1 | Expression of myofibroblast markers by TAMs in PDAC

PDAC is characterized by extensive fibrosis, and studies have widely adopted α SMA assessment approaches to evaluate the degree of fibrosis in cancers, including PDAC.

To investigate whether monocytes/macrophages can transdifferentiate into (myo)fibroblasts in PDAC, we first examined the distribution of TAMs and CAFs in paraffin-embedded tissues derived from PDAC patients. We adopted two-color IF and detected intermediate cells that uniquely co-expressed a pan-macrophage marker (CD68) and a

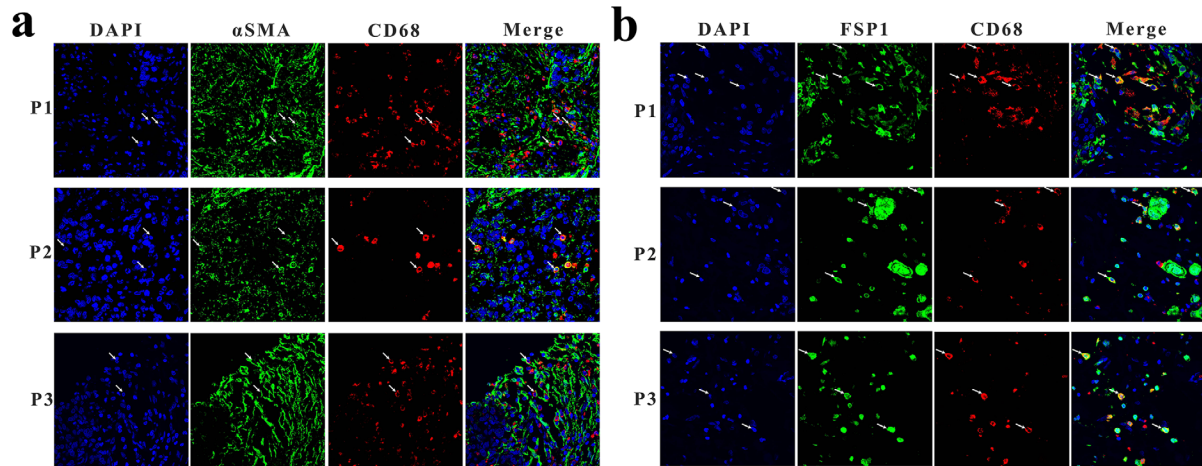


FIGURE 1 Expression of myofibroblast markers by TAMs in PDAC. A, Immunofluorescence staining for α SMA (green), CD68 (red), and DAPI (blue, for nuclear staining) in PDAC tissues of three patients (P1, P2, and P3). B, Immunofluorescence staining for FSP1 (green), CD68 (red), and DAPI (blue, for nuclear staining) in PDAC tissues of three patients (P1, P2, and P3)

Abbreviations: TAMs, tumor associated macrophages; PDAC, pancreatic ductal adenocarcinoma; DAPI, 4',6-diamidino-2-phenylindole; FSP1, fibroblast-specific protein 1.

myofibroblast marker (α SMA) in PDAC tissue (Figure 1A) but not in normal pancreas tissue (data not shown). In addition, we detected colocalization of CD68 and FSP1 in PDAC tissue, suggesting that monocytes/macrophages contribute to FSP1 expression (Figure 1B).

3.2 | Oxidative stress induced MMT in vitro

Because the precision of above analysis was limited owing to the close proximity of TAMs and CAFs in the stroma, we isolated fibroblasts in vitro³⁵ and found that CAFs expressed higher levels of α SMA than NFs (Figure 2A). In addition, exogenous stimulation with TGF- β 1 induced α SMA expression by both NFs and CAFs. However, these cells did not express CD68, as assessed by WB or IF (Figures 2A, S1A, and S1B).

In addition, considering that macrophages have phagocytic capacity, to exclude the possibility of macrophages phagocytosing α SMA⁺ cells or debris, we isolated fresh human blood monocytes (>95% were CD14⁺; Figure S1C) from PBMCs. WB result showed that monocytes expressed almost no α SMA, fibronectin, or vimentin but did express FSP1. After differentiation in vitro (7 days, without other stimuli), most cells were fried egg shaped with a few being spindle shaped (Figure 2B), and cells started to express α SMA at a relatively low level (Figures 2C and 2E).

Then we explored the underlying mechanisms of α SMA expression. First, we speculated that cytokines secreted from PDAC cancer cells may play a role in MMT. However, compared with DMEM, supernatant from pancreatic cancer cells or HPDE6-C7 had no obvious effect on α SMA expression by monocytes/macrophages (Figure S2A). Second, TGF- β 1

is the primary cytokine initiating fibrosis in many organs but did not obviously affect MMT (Figure S2B). Because ROS were generated during monocyte-to-macrophage differentiation, and macrophages expressed α SMA at a low level, we speculated that ROS were the primary cause of α SMA expression. Monocytes are vulnerable to oxidative stress,⁴¹ and H₂O₂ has been regularly adopted to assess the effects of oxidative stress. In this study, we performed a CCK-8 assay to demonstrate short-term (1 day) and long-term (7 days) cytotoxicity (Figure 2D) and demonstrated that H₂O₂ concentrations generally not exceeding 100 μ M were relatively nontoxic to monocytes/macrophages.

H₂O₂ significantly induced α SMA RNA and protein expression in a time- and concentration-dependent manner (Figures 2E and 2F), suggesting that α SMA expression was regulated at the transcriptional level. Although α SMA expression in H₂O₂-treated monocytes was lower than that in pancreatic fibroblasts, it was much higher than that in AsPC-1, BXPC-3, CFPAC-1, PANC-1, and HPDE6-C7 (data not shown). Additionally, we demonstrated upregulated α SMA expression by single cell and morphological changes, with H₂O₂-treated cells being spindle shaped (Figure 2G).

Other markers of myofibroblasts include fibronectin, Col1, and FSP1. In this study, we found that monocytes expressed high levels of FSP1; however, after differentiation in vitro, the expression of FSP1 in HMDMs decreased (Figure 2E). Regarding the secreted proteins fibronectin and Col1, freshly isolated monocytes expressed no fibronectin or Col1, and cells cultured in vitro started to express fibronectin (Figure S2C) but not Col1; however, the effect of H₂O₂ on fibronectin expression varied among cells from different donors, and the difference in mRNA (Figure 2I) or protein (Figures 2E, 2H, and 2J) levels did not reach statistical significance.

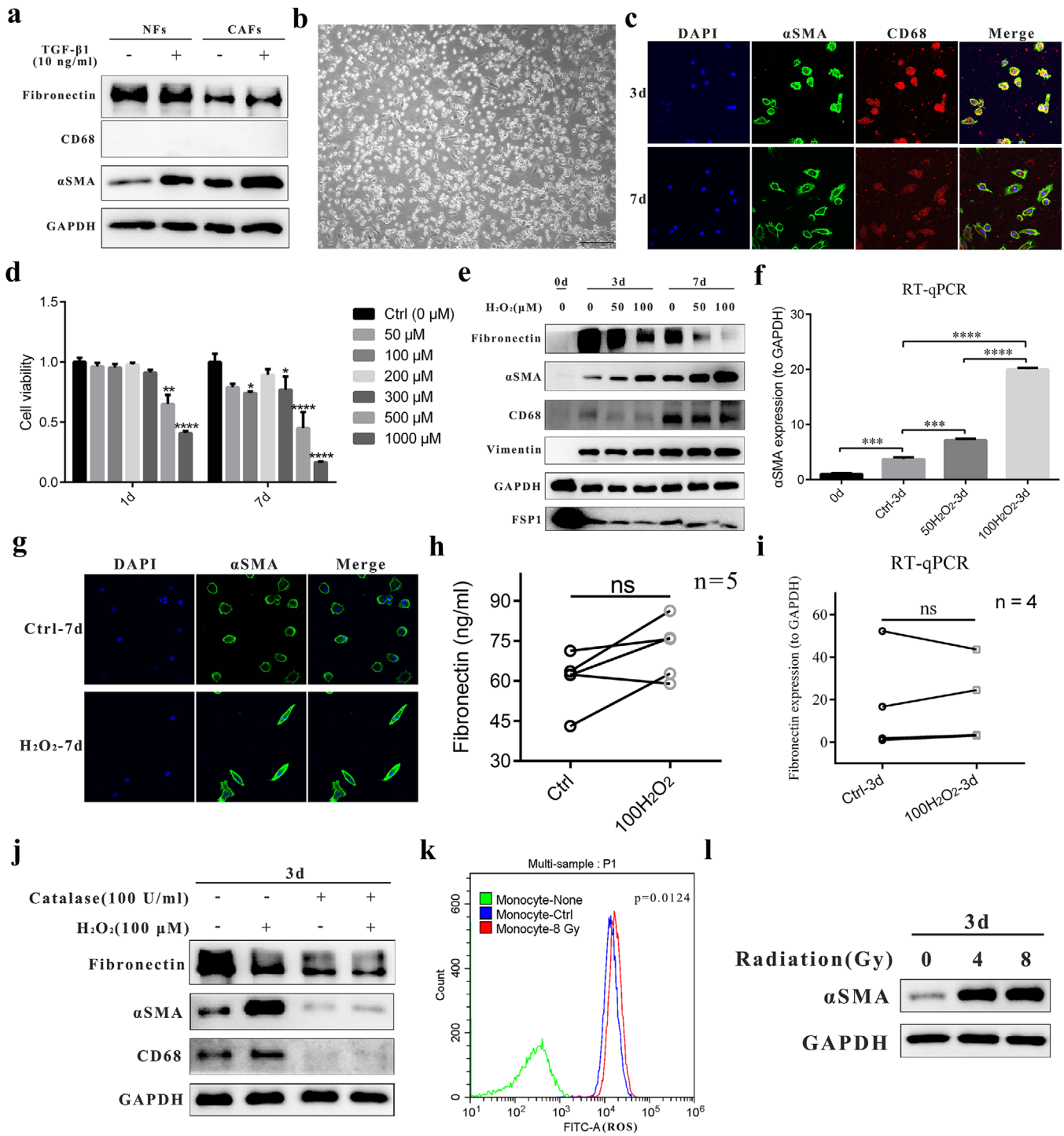


FIGURE 2 Oxidative stress induced MMT in vitro. A, Western blot analysis of fibronectin, CD68, and α SMA expression (3 days). GAPDH was used as the loading control. B, Representative photograph of human monocyte-derived macrophages cultured in vitro (7 days). C, Representative immunofluorescence staining for α SMA (green), CD68 (red), and DAPI (blue, for nuclear staining) in monocytes cultured for 3 or 7 days in vitro. D, A CCK-8 assay was used to evaluate the cytotoxicity of H_2O_2 to monocytes cultured in vitro for 1 or 7 days. Data from one representative donor of three donors are shown. Two-way ANOVA followed by Bonferroni's post hoc test was used to evaluate the significance of the differences between the experimental and ctrl groups. E, Western blot analysis of α SMA, vimentin, FSP1, and CD68 expression. GAPDH was used as the loading control. F, Reverse transcription-quantitative polymerase chain reaction (RT-qPCR) measurement of α SMA gene expression levels. GAPDH was used as the loading control. One-way ANOVA followed by Bonferroni's post hoc test was used to evaluate the significance of the differences between the groups. G, Immunofluorescence staining for α SMA (green), CD68 (red), and DAPI (blue, for nuclear staining) in macrophages treated or not with treated $100 \mu M H_2O_2$. Cells treated with H_2O_2 tended to be spindle shaped. H, ELISA of fibronectin concentrations in supernatants from monocytes treated or not treated with $100 \mu M H_2O_2$ ($n = 5$). A paired t -test was used for comparisons. I, RT-qPCR measurement of fibronectin gene

In addition, as shown in Figure 2J, after the addition of catalase, a key antioxidant enzyme responsible for the conversion of H_2O_2 to water and oxygen, monocytes/macrophages did not express α SMA, and catalase neutralized the effect of H_2O_2 on α SMA expression. In addition, CD68 was also not expressed in the catalase-treated group, indicating that a low concentration of H_2O_2 (ie, ROS) was important for monocyte-to-macrophage differentiation. Intriguingly, catalase almost completely inhibited fibronectin production, as demonstrated by RT-qPCR, ELISA (data not shown) and WB (Figure 2J), suggesting that basal H_2O_2 production was necessary for fibronectin generation.

Finally, to more accurately and precisely confirm the effect of oxidative stress, we adopted another method of oxidative stress induction, radiation, to verify the role of ROS in MMT.⁴² Radiation exhibited different levels of cytotoxicity to different donors (Figure S2D) and induced ROS production in monocytes (8 Gy; Figure 2K). As shown in Figure 2L, radiation increased α SMA expression, and this increase was also inhibited by catalase (data not shown).

3.3 | MMT inhibited the phagocytic function of monocytes/macrophages

Macrophages are innate immunocytes with phagocytic capacity; however, fibroblasts are generally thought to have no capacity for phagocytosis. Therefore, we evaluated the changes in phagocytic capacity during MMT. We used latex beads and found that treatment with 100 μ M H_2O_2 significantly reduced the functional phagocytic capacity, as indicated by the phagocytic activity (Figure 3, $P < .001$).

3.4 | The p53 stabilizer nutlin-3 induced MMT through ROS generation but not through the p53 transcription/mitochondria-dependent signaling pathway

First, we performed RNA sequencing (RNA-seq) to identify DEGs between the groups of cells treated or not treated with H_2O_2 (Table S2), including α SMA (Fold change, 2.98; P

= .036), and signaling pathways involved in MMT. In Figure 4A, the heatmap illustrates DEGs between the two group of cells and the volcano plot shows 68 upregulated genes and 26 downregulated genes in H_2O_2 -treated monocytes. In addition, we used KEGG analysis to screen the pathways enriched in the DEGs and found that H_2O_2 regulates the p53 pathway.

Second, through WB analysis, we demonstrated that H_2O_2 increased the expression of p53 and the target genes p21 and MDM2 in a time- and concentration-dependent manner (Figure 4B); the same trend was observed for radiation (Figure 4C). Consistent with the results of a previous study,⁴³ the p53 stabilizer nutlin-3 upregulated α SMA expression in monocytes (Figure 4D). Although reports have indicated that α SMA is a transcriptional target of p53⁴⁴ and that p53 can increase ROS production through a mitochondrial pathway,^{45,46} neither PFT- α (10 μ M) nor PFT- μ (2 or 5 μ M) reduced α SMA expression induced by H_2O_2 or nutlin-3 (Figures 4D and 4E), even at concentrations as high as 50 μ M. Besides that, we demonstrated that nutlin-3 induced ROS production in human monocytes (Figure 4F), and catalase addition reduced the α SMA expression induced by nutlin-3 but had little effect on p53, p21, or MDM2 expression (Figure 4G).

3.5 | ROS induced MMT through the p38-mitogen-activated protein kinase (MAPK) signaling pathway

Other studies showed that ROS can activate MAPKs in monocytes,¹⁸ and gene ontology analysis of RNA-seq data identified MAPK kinase activation by H_2O_2 (data not shown). We pretreated monocytes with different MAPK inhibitors and found that only the p38 inhibitor SB203580 had an inhibitory effect on ROS-induced MMT. In this study, we found that 100 μ M H_2O_2 activated p38 in 30 min, with the activation peak at 10-15 min (Figure 5A). As for Nutlin-3 (10 μ M) also activated p38 in 30 min, but the activation peaked relatively later than for H_2O_2 (Figure 5B). Nutlin-3 was dissolved in DMSO, and the same volume of DMSO had little effect on p38 activation (data not shown). In addition, radiation (8 Gy) activated p38 in 30 min (Figure 5C).

expression levels ($n = 4$). The Wilcoxon matched-pairs test was used for comparison. J, Western blot analysis of fibronectin, α SMA, and CD68 expression in monocytes treated with H_2O_2 (100 μ M, \pm) or the H_2O_2 -scavenging enzyme catalase (100 U/mL, \pm) on day 3. GAPDH was used as the loading control. K, Flow cytometric analysis of intracellular ROS levels in monocytes irradiated with 8 Gy or sham-irradiated, using H2DCFDA fluorescent probe (green, without probe; blue, sham-irradiated; red, irradiated with 8 Gy). A paired t -test was used for comparisons between Ctrl and 8 Gy groups ($n = 3$). L, Western blot analysis of α SMA expression on day 3 after irradiation (0/4/8 Gy). GAPDH was used as the loading control. The data are expressed as the means \pm standard errors of the mean and are representative of at least three experiments. Abbreviations: MMT, monocyte-to-myofibroblast transdifferentiation; NFs, normal fibroblasts; CAFs, cancer associated fibroblasts; DAPI, 4',6-diamidino-2-phenylindole; FSP1, fibroblast-specific protein 1; RT-qPCR, reverse transcription-quantitative polymerase chain reaction; ELISA, enzyme-linked immunosorbent assay; ns, not significant ($P > .05$).

* $P < .05$; *** $P < .001$; **** $P < .0001$.

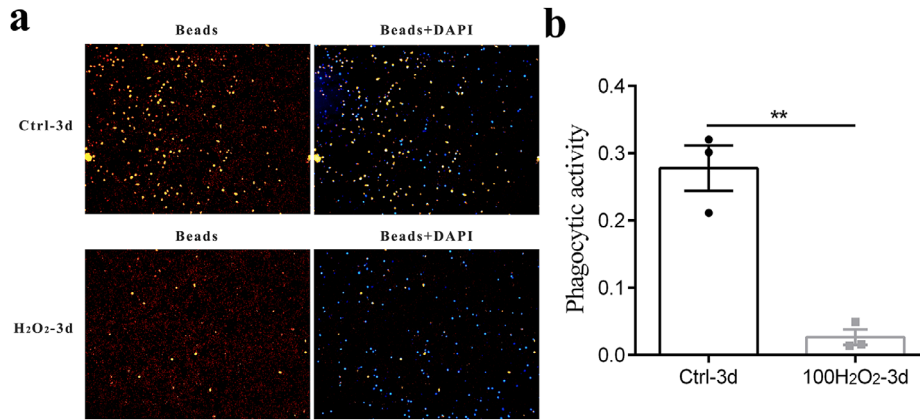


FIGURE 3 MMT inhibited the phagocytic function of monocytes/macrophages. A, Representative immunofluorescence images showing phagocytosis of latex beads (red) by monocytes treated or not treated with 100 μM H_2O_2 for 3 days. Nuclei were counterstained with DAPI (blue). B, Phagocytic capacity was quantified by measuring phagocytic activity (the number of beads divided by the number of nuclei) ($n = 3$). The data are expressed as the means \pm standard errors of the mean. A paired t -test was used for comparisons

Abbreviations: MMT, monocyte-to-myofibroblast transdifferentiation; DAPI, 4',6-diamidino-2-phenylindole.

** $P < .01$

However, the p38 inhibitor SB203580 (1-2 μM) partially but not completely inhibited αSMA expression induced by H_2O_2 , nutlin-3, or radiation (Figure 5D), suggesting that other pathways may also participate in the induction of αSMA expression during MMT.

3.6 | MMT generated a unique subset of myofibroblasts in PDAC and promoted the proliferation of PDAC cells

To date, studies have shown that CAFs in the tumor milieu are heterogeneous, and increasing attention has been devoted to identifying new markers expressed by special subtypes of CAFs. In this study, we aimed to more precisely define the characteristics of these transdifferentiated cells.

Other studies identified a new subset of CAFs with characteristics of inflammatory cells, termed inflammatory cancer-associated fibroblasts (iCAFs), in PDAC.⁴⁷ Thus, we hypothesized that MMT may produce CAFs similar to those in this newly identified subset. Supernatant from these MMT cells promoted the proliferation of AsPC-1 cells (Figure 6) but had little effect on BxPC-3, CFPAC-1, or PANC-1 cells (data not shown).

4 | DISCUSSION

The accurate definition of fibroblasts is incompletely elucidated. Fibroblasts are large spindle-shaped cells but no single fibroblast-specific immunocytochemical marker has been identified; therefore, several markers, including αSMA , FSP1, FAP, Col1, and fibronectin, are combined to distinguish them.

Similarly, the CAFs in PDAC are heterogeneous with different markers.^{10,48} The same characteristic applies to the numerous origins of CAFs, and accumulating evidence indicates that normal resident fibroblasts, fibrocytes, MSCs, adipocytes, and cancer cells can transdifferentiate into fibroblasts in different types of cancer.^{11,12}

A previous report demonstrated that mouse aortic smooth muscle cells transdifferentiated into a macrophage-like state after cholesterol loading; this transdifferentiation was accompanied by decreased protein levels of αSMA and increased levels of CD68 and Mac-2.²⁴ Many studies have reported that TGF- β 1 can induce macrophage-to-myofibroblast transition in a kidney injury mouse model^{32,49} and that monocytes can transdifferentiate into vascular endothelial cells⁵⁰ or neuronal-like cells.⁵¹ Here, we found for the first time that oxidative stress can induce MMT.

First, through IF we found costaining of αSMA with CD68 in PDAC tissues (Figure 1A), but αSMA expression in these cells was relatively lower than that in other CAFs. This expression pattern explained why only a few cells co-expressed αSMA and CD68 in PDAC tissue as assessed by IF, considering that monocytes/macrophages cultured in vitro broadly expressed αSMA (Figures 2C and 2E). Consistent with another study showing that FSP1 could identify an inflammatory subpopulation of macrophages in the liver,²⁹ we found that FSP1 colocalized broadly with CD68 in PDAC tissues (Figure 1B). In addition, through WB analysis, we found that freshly isolated human monocytes expressed high levels of FSP1 but that FSP1 expression declined during monocyte-to-macrophage differentiation (Figure 2E).

Ludin et al previously reported that monocytes/macrophages express αSMA , which preserves primitive hematopoietic cells in the bone marrow.⁵² Other studies

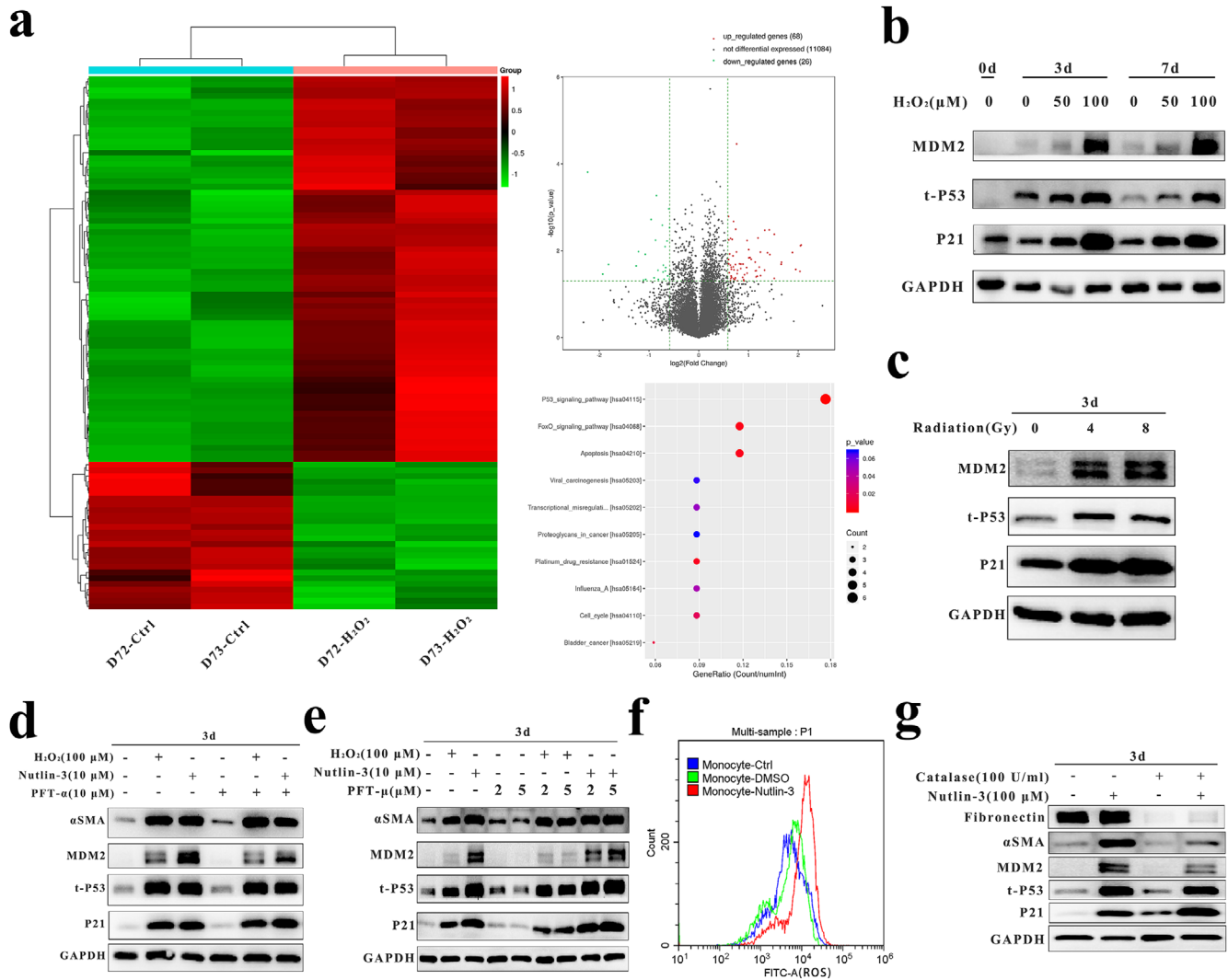


FIGURE 4 The p53 stabilizer nutlin-3 induced MMT through ROS generation but not through the p53 transcription/mitochondria-dependent signaling pathway. A, RNA-seq analysis of monocytes obtained from two healthy donors (D72 and D73), and treated or not treated with 100 μM H₂O₂ for 7 days. The heatmap shows hierarchical clustering of mRNA levels of genes in monocytes treated as indicated; the volcano plot shows differentially expressed genes plotted as the log₂(fold change) versus the -log₁₀(P-value). A total of 94 differentially expressed genes between the H₂O₂-treated cell group and the control cell group exceeded the established thresholds (-log₁₀(P-value) > 1.30 and log₂-fold change > .585; upregulated genes are shown in red, and downregulated genes are shown in green). KEGG pathway analysis was performed on the upregulated genes identified by RNA-seq. B and C, Western blot analysis of the expression of p53 and the target genes p21 and MDM2 in freshly isolated monocytes (0 day), monocytes treated with 0/50/100 μM H₂O₂ for 3/7 days, and monocytes treated with radiation (0/4/8 Gy) for 3 days. GAPDH was used as the loading control. D and E, Western blot analysis of the expression of αSMA, p53, p21, and MDM2 in monocytes treated or not treated with nutlin-3, H₂O₂, PFT-α, or PFT-μ. GAPDH was used as the loading control. F, Representative flow cytometric analysis of intracellular ROS levels in monocytes treated or not treated with nutin-3 (10 μM) or the same volume of DMSO (blue, ctrl; green, DMSO; red, nutlin-3). G, Western blot analysis of monocytes treated or not treated with 10 μM nutlin-3 or 100U/mL catalase. GAPDH was used as the loading control. Data are representative of three experiments

Abbreviations: MMT, monocyte-to-myfibroblast transdifferentiation; RNA-seq, RNA sequencing; DEGs, differentially expressed genes; KEGG, Kyoto Encyclopedia of Genes and Genomes; DMSO, dimethyl sulfoxide.

demonstrated that TGF-β1-SMAD3 can induce MMT (αSMA and Col1 expression) in fibrotic diseases such as renal fibrosis.³² However, we found that TGF-β1 activated fibroblasts (Figure 2A) but did not induce MMT in vitro (Figure S2B), as demonstrated also by another study.⁴³ In addition, we found that αSMA expression by monocytes was

not increased by exposure to tumor supernatant (Figure S2A). Intriguingly, although another study identified fibronectin expression in macrophages,⁵³ we demonstrated here that monocytes began to express fibronectin but not Col1 upon differentiation to macrophages in vitro (Figures 2E and S2C), similar to the results of other studies demonstrating that

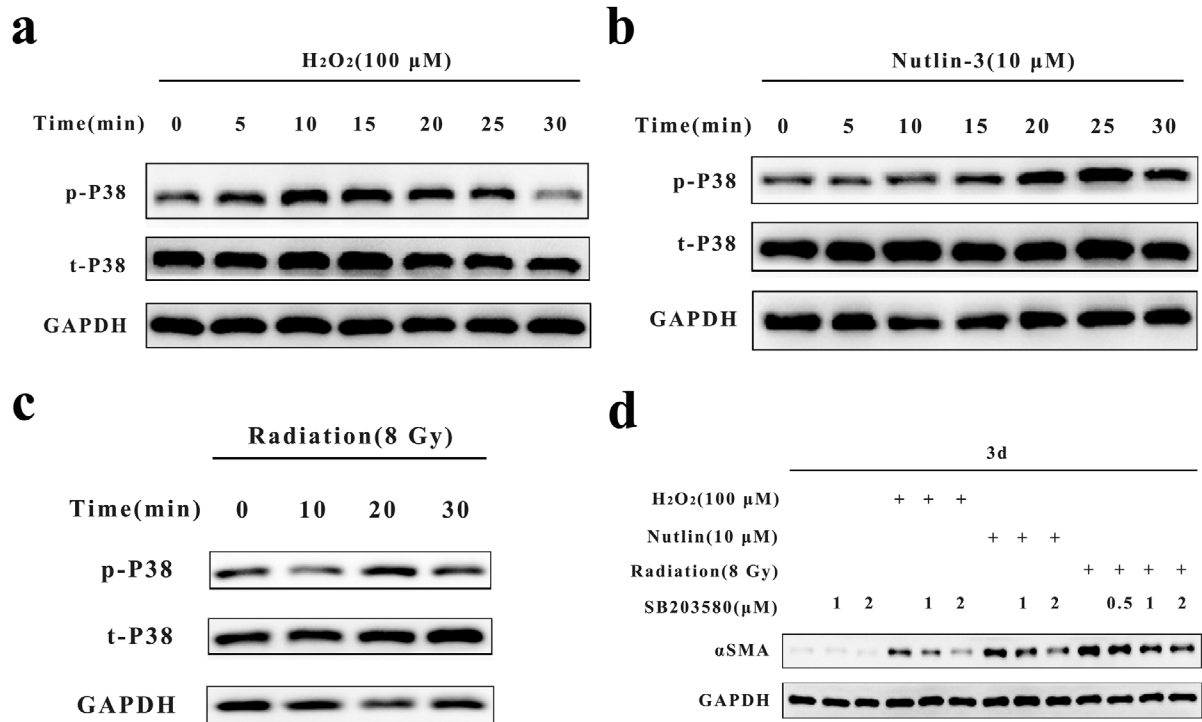


FIGURE 5 ROS induced MMT through p38-MAPK signaling pathway. A-C, Western blot analysis of p-p38 and t-p38 expression in monocytes treated with H_2O_2 (100 μM), nutlin-3 (10 μM), or radiation (8 Gy) at different time points (≤ 30 min). GAPDH was used as the loading control. D, Western blot analysis of αSMA expression in monocytes treated with H_2O_2 (100 μM), nutlin-3 (10 μM), or radiation (8 Gy) and the p38 inhibitor SB203580 (0/0.5/1/2 μM). GAPDH was used as the loading control. Data are representative of three experiments

Abbreviations: MAPK, mitogen-activated protein kinase.

tissue-resident macrophages of embryonic origin produced much more Col1 than HMDMs in PDAC,⁵⁴ and these $CD68^+Col1^-$ cells excluded the potential contamination with bone marrow-derived fibrocytes.

Because ROS generation was low and αSMA was slightly upregulated during monocyte-to-macrophage differentiation, we speculated and demonstrated that ROS can increase the expression of αSMA by monocytes in vitro (Figure 2E). H_2O_2 is generally adopted to assess the effects of oxidative stress, and previous studies have detected the cytotoxicity of H_2O_2 to monocytes; however, the most commonly used interval was limited to 24 h.¹⁸ Therefore, we performed a CCK-8 assay to demonstrate both short-term (1 day) and long-term (7 days) cytotoxicity and found that H_2O_2 concentrations generally not exceeding 100 μM were relatively nontoxic to monocytes/macrophages (Figure 2D). Furthermore, radiation was used to verify the role of ROS in MMT (Figure 2L), which could partially explain the radiation-induced fibrosis in PDAC observed clinically.⁵⁵ The contradiction between our results and those of previous studies⁴⁹ may be explained by the fact that others explored the mechanisms mainly in mouse model of renal fibrosis, whereas we mainly used freshly isolated human monocytes cultured in vitro.

Additionally, previous studies have shown that moderate ROS levels are essential for monocyte-to-macrophage

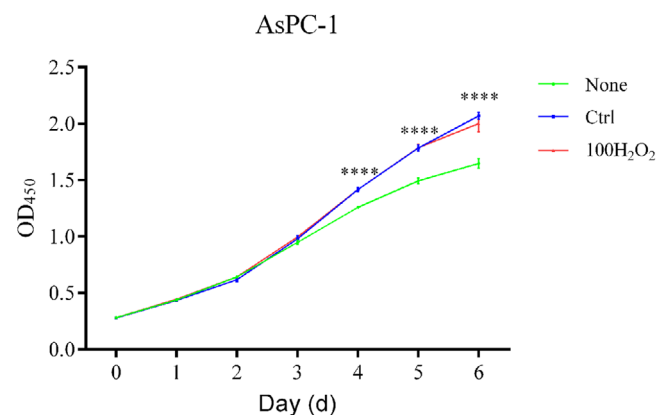


FIGURE 6 MMT generated a subset of myofibroblasts promoting the proliferation of cancer cells in PDAC.

A CCK-8 assay was used to evaluate the proliferation of cancer cells (AsPC-1) cultured with DMEM or supernatant (30%) from monocytes treated or not treated with 100 μM H_2O_2 . Data are expressed as the means \pm standard errors of the mean ($n = 3$). Two-way ANOVA followed by Bonferroni's post hoc test was used to evaluate the significance of differences among the groups. The asterisks indicate a significant difference between the "100 H_2O_2 " and "None" groups

Abbreviations: MMT, monocyte-to-myofibroblast transdifferentiation; PDAC, pancreatic ductal adenocarcinoma.

**** $P < .0001$

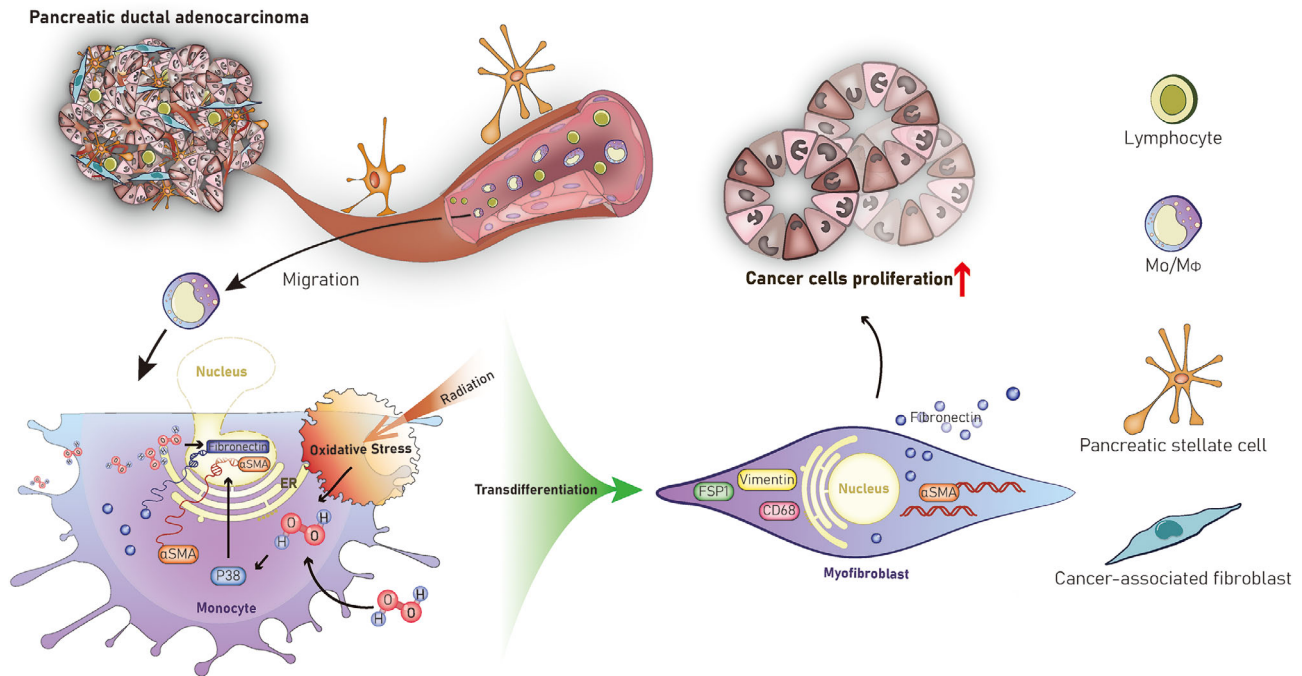


FIGURE 7 Schematic diagram of ROS-dependent MMT in PDAC. Monocytes in human blood are recruited into PDAC tissues. Low intracellular levels of H_2O_2 are important for fibronectin mRNA synthesis, protein expression, and secretion in monocytes and macrophages. Oxidative stressors, such as radiation, can reduce the phagocytic capacity and simultaneously activate the p38-MAPK signaling pathway, thus inducing α SMA mRNA and protein expression in monocytes/macrophages. However, these cells do not express Col1. Therefore, myofibroblasts transdifferentiated from monocytes are characterized by low phagocytic capacity; high α SMA/Col1 levels; fibronectin, vimentin, FSP1, and CD68 expression; and features of inflammatory cells. In addition, supernatant from these cells can stimulate cancer cell (AsPC-1) proliferation, thus promoting tumor progression in PDAC.

Abbreviations: MMT, monocyte-to-myofibroblast transdifferentiation; PDAC, pancreatic ductal adenocarcinoma; MAPK, mitogen-activated protein kinase; Col1, collagen 1.

differentiation and phagocytic capacity of macrophages.¹⁶ In this study, we found a lack of expression of the macrophage differentiation marker CD68 after the addition of catalase (Figure 2J) and a significant reduction in phagocytic capacity during MMT induced by H_2O_2 (Figure 3), indicating an unfavorable effect of excessive ROS on the phagocytic function of macrophages. These results were consistent with those of a recently published study showing that macrophages can utilize excess ROS to stiffen the cytoplasm and reduce their phagocytic propensity,⁵⁶ identifying ROS as a double-edged sword in monocytes/macrophages.

Besides that, we identified DEGs through RNA-seq and found that ROS can activate p53 (Figure 4A-C). A previous study showed that nutlin-3 can induce morphological changes and α SMA expression in human primary monocytes.⁴³ PFT- α has been reported to be a selective inhibitor of p53-mediated transcription in the nucleus; PFT- μ inhibits p53 binding to mitochondrial proteins. However, in our study, we demonstrated the role of nutlin-3 in inducing α SMA expression, but neither PFT- α nor PFT- μ inhibited this MMT (Figures 4D and 4E), suggesting that nutlin-3 induces MMT through a pathway other than the p53 transcription/mitochondria-dependent signaling pathway. Another study reported that

nutlin-3 can induce ROS generation independent of the p53 status.⁵⁷ In this study, we also demonstrated that nutlin-3 promoted ROS generation in monocytes and that catalase inhibited nutlin-3-induced MMT (Figures 4F and 4G). However, we did not knock down p53 due to the low transfection efficiency of primary human monocytes, as also reported by others⁵⁸; therefore, the precise mechanisms of nutlin-3 or p53 in MMT merit further study.

In consistency with the results of other studies,¹⁸ we found that ROS can activate p38 in monocytes. Moreover, the p38 inhibitor SB203580 partially but not completely inhibited MMT (Figure 5), demonstrating that p38 plays a major role in the MMT process. However, other mechanisms may exist that need to be investigated.

In PDAC, ECM is a product of activated PSCs; however, the activity of PSCs as evaluated by α SMA expression is not always associated with the status of fibrosis,⁵⁹ because α SMA expression is a more favorable marker for PSCs differentiation than for PSCs activity. The activated stroma index, that is, the ratio of the α SMA-stained area to the Col1-stained area, is a novel index and has been used to classify PDAC into four types with significantly different overall survival: dormant (low α SMA/high Col1), inert (low α SMA/low

Col1), fibrogenic (high α SMA/high Col1), and fibrolytic (high α SMA/low Col1) PDAC.^{60,61} Our results demonstrated MMT with elevated expression of α SMA and fibronectin but not Col1, suggesting that MMT contributes to the fibrolytic type, which has the worst prognosis among these types.

CAFs in PDAC are heterogeneous. David et al identified two distinct CAFs subtypes in PDAC: iCAFs, which lack elevated α SMA expression and instead express inflammatory markers such as IL-6 and leukemia inhibitory factor and are located farther away from tumor cells; and myofibroblastic CAFs, which express markers of myofibroblasts, such as α SMA, and are found adjacent to tumor cells.^{47,48} Recently, this group found another subtype of CAFs, antigen-presenting CAFs, which express major histocompatibility complex class II and CD74 molecules but not classical costimulatory molecules.⁶² However, these studies have precluded CD45⁺ immune cells at isolating CAFs for single-cell RNA-seq. In our study, through RNA-seq, we defined MMT cells as another type of CAFs, with characteristics of macrophages, in PDAC (Table S2). For example, we recently identified CD10 expression by monocytes or macrophages in PDAC,³⁴ and other researchers have reported that CD10⁺ CAFs can promote the progression of PDAC and breast cancer.^{63,64} In summary, MMT promotes the production of CD10⁺ α SMA⁺ cells in cancers.

Finally, we explored the effect of MMT on cancer cells and found that supernatant from MMT cells could promote the proliferation of AsPC-1 cells (Figure 6) but had little effect on other PDAC cancer cell lines, which may be attributed to the limited amount of freshly isolated monocytes and thus the low levels of cytokines in the supernatant. However, we did not conduct animal experiment, compare gene expression between monocyte-derived myofibroblasts and PSC-derived myofibroblasts, or explore the prognostic value of MMT, which needs further investigation in the future.

In conclusion, oxidative stress in the extracellular tumor microenvironment or inside cells could induce MMT in PDAC, thus inducing reactive stroma and modulating immunosuppression (Figure 7). Reducing oxidative stress may be a promising future therapeutic regimen, because other studies have found that antioxidant therapy blocks TAMs differentiation and tumorigenesis in mouse models of cancer.¹⁶

AVAILABILITY OF DATA AND MATERIALS

The data that support the findings of this study are available from the corresponding author upon reasonable request.

CONFLICT OF INTEREST

The authors declare no conflict of interest.

FUNDING INFORMATION

This work was supported by grants from the National Natural Science Foundation of China (No. 81672390) and

the National Key Research and Development Plan (No. 2017YFC0910002).

AUTHOR CONTRIBUTIONS

XH and SL conceived and designed the study. CH, XH, AK, YM, SS, FD, and JW contributed to data collection, management and statistics, and participated in results analysis and article modification. XH and CH drafted the manuscript. PH and SL revised the manuscript. All authors read and approved the final manuscript.

ORCID

Xin Huang  <https://orcid.org/0000-0002-0359-7290>

Shengping Li  <https://orcid.org/0000-0002-2698-2757>

REFERENCES

1. Siegel RL, Miller KD, Jemal A. Cancer statistics. *CA Cancer J Clin.* 2019;69(1):7-34.
2. Rahib L, Smith BD, Aizenberg R, Rosenzweig AB, Fleshman JM, Matrisian LM. Projecting cancer incidence and deaths to 2030: the unexpected burden of thyroid, liver, and pancreas cancers in the United States. *Cancer Res.* 2014;74(11):2913-2921.
3. Henriksen A, Dyhl-Polk A, Chen I, Nielsen D. Checkpoint inhibitors in pancreatic cancer. *Cancer Treat Rev.* 2019;78:17-30.
4. Wu AA, Jaffee E, Lee V. Current status of immunotherapies for treating pancreatic cancer. *Curr Oncol Rep.* 2019;21(7):60.
5. Waltregny D, Glenisson W, Tran SL, et al. Histone deacetylase HDAC8 associates with smooth muscle alpha-actin and is essential for smooth muscle cell contractility. *FASEB J.* 2005;19(8):966-968.
6. Hwang RF, Moore T, Arumugam T, et al. Cancer-associated stromal fibroblasts promote pancreatic tumor progression. *Cancer Res.* 2008;68(3):918-926.
7. Ozdemir BC, Pentcheva-Hoang T, Carstens JL, et al. Depletion of carcinoma-associated fibroblasts and fibrosis induces immunosuppression and accelerates pancreas cancer with reduced survival. *Cancer Cell.* 2014;25(6):719-734.
8. Kim EJ, Sahai V, Abel EV, et al. Pilot clinical trial of hedgehog pathway inhibitor GDC-0449 (vismodegib) in combination with gemcitabine in patients with metastatic pancreatic adenocarcinoma. *Clin Cancer Res.* 2014;20(23):5937-5945.
9. Rhim AD, Oberstein PE, Thomas DH, et al. Stromal elements act to restrain, rather than support, pancreatic ductal adenocarcinoma. *Cancer Cell.* 2014;25(6):735-747.
10. Helms E, Onate MK, Sherman MH. Fibroblast heterogeneity in the pancreatic tumor microenvironment. *Cancer Discov.* 2020. <https://doi.org/10.1158/2159-8290.CD-19-1353>
11. Cirri P, Chiarugi P. Cancer associated fibroblasts: the dark side of the coin. *Am J Cancer Res.* 2011;1(4):482-497.
12. Omary MB, Lugea A, Lowe AW, Pandol SJ. The pancreatic stellate cell: a star on the rise in pancreatic diseases. *J Clin Invest.* 2007;117(1):50-59.
13. Waghray M, Yalamanchili M, Dziubinski M, et al. GM-CSF mediates mesenchymal-epithelial cross-talk in pancreatic cancer. *Cancer Discov.* 2016;6(8):886-899.
14. Protti MP, De Monte L. Immune infiltrates as predictive markers of survival in pancreatic cancer patients. *Front Physiol.* 2013;4:210.

15. Trachootham D, Lu W, Ogasawara MA, Valle NR-D, Huang P. Redox regulation of cell survival. *Antioxid Redox Signaling*. 2008;10(8):1343-1374.
16. Zhang Y, Choksi S, Chen K, Pobezińska Y, Linnoila I, Liu ZG. ROS play a critical role in the differentiation of alternatively activated macrophages and the occurrence of tumor-associated macrophages. *Cell Res*. 2013;23(7):898-914.
17. Lehoux G, Le Gouill C, Stankova J, Rola-Pleszczynski M. Upregulation of expression of the chemokine receptor CCR5 by hydrogen peroxide in human monocytes. *Mediators Inflamm*. 2003;12(1):29-35.
18. Tang DL, Shi YZ, Kang R, et al. Hydrogen peroxide stimulates macrophages and monocytes to actively release HMGB1. *J Leukoc Biol*. 2007;81(3):741-747.
19. Roux C, Jafari SM, Shinde R, et al. Reactive oxygen species modulate macrophage immunosuppressive phenotype through the up-regulation of PD-L1. *Proc Natl Acad Sci USA*. 2019;116(10):4326-4335.
20. Chen X, Song E. Turning foes to friends: targeting cancer-associated fibroblasts. *Nat Rev Drug Discov*. 2019;18(2):99-115.
21. Jopling C, Boue S, Belmonte JCI. Dedifferentiation, transdifferentiation and reprogramming: three routes to regeneration. *Nat Rev Mol Cell Biol*. 2011;12(2):79-89.
22. Tanabe K, Ang CE, Chanda S, et al. Transdifferentiation of human adult peripheral blood T cells into neurons. *Proc Natl Acad Sci USA*. 2018;115(25):6470-6475.
23. Di Tullio A, Vu Manh TP, Schubert A, Castellano G, Mansson R, Graf T. CCAAT/enhancer binding protein alpha (C/EBP(alpha))-induced transdifferentiation of pre-B cells into macrophages involves no overt retrodifferentiation. *Proc Natl Acad Sci USA*. 2011;108(41):17016-17021.
24. Rong JX, Shapiro M, Trogan E, Fisher EA. Transdifferentiation of mouse aortic smooth muscle cells to a macrophage-like state after cholesterol loading. *PNAS*. 2003;100(23):13531-13536.
25. Feng R, Desbordes SC, Xie HF, et al. PUA and C/EBP alpha/beta convert fibroblasts into macrophage-like cells. *PNAS*. 2008;105(16):6057-6062.
26. Jiang H, Hegde S, DeNardo DG. Tumor-associated fibrosis as a regulator of tumor immunity and response to immunotherapy. *Cancer Immunol Immunother*. 2017;66(8):1037-1048.
27. Shi C, Washington MK, Chaturvedi R, et al. Fibrogenesis in pancreatic cancer is a dynamic process regulated by macrophage-stellate cell interaction. *Lab Invest*. 2014;94(4):409-421.
28. Li N, Li Y, Li Z, et al. Hypoxia inducible factor 1 (HIF-1) recruits macrophage to activate pancreatic stellate cells in pancreatic ductal adenocarcinoma. *Int J Mol Sci*. 2016;17(6):799.
29. Osterreicher CH, Penz-Osterreicher M, Grivninkov SI, et al. Fibroblast-specific protein 1 identifies an inflammatory subpopulation of macrophages in the liver. *Proc Natl Acad Sci USA*. 2011;108(1):308-313.
30. Tchou J, Zhang PJ, Bi Y, et al. Fibroblast activation protein expression by stromal cells and tumor-associated macrophages in human breast cancer. *Hum Pathol*. 2013;44(11):2549-2557.
31. Afik R, Zigmond E, Vugman M, et al. Tumor macrophages are pivotal constructors of tumor collagenous matrix. *J Exp Med*. 2016;213(11):2315-2331.
32. Nikolic-Paterson DJ, Wang S, Lan HY. Macrophages promote renal fibrosis through direct and indirect mechanisms. *Kidney Int*. 2014;4(1):34-38.
33. Toullec A, Gerald D, Despouy G, et al. Oxidative stress promotes myofibroblast differentiation and tumour spreading. *EMBO Mol Med*. 2010;2(6):211-230.
34. Huang X, He C, Lin G, et al. Induced CD10 expression during monocyte-to-macrophage differentiation identifies a unique subset of macrophages in pancreatic ductal adenocarcinoma. *Biochem Biophys Res Commun*. 2020;524(4):1064-1071.
35. Bachem MG, Schunemann M, Ramadani M, et al. Pancreatic carcinoma cells induce fibrosis by stimulating proliferation and matrix synthesis of stellate cells. *Gastroenterology*. 2005;128(4):907-921.
36. Mao Y, Huang X, Shuang Z, et al. PARP inhibitor olaparib sensitizes cholangiocarcinoma cells to radiation. *Cancer Med*. 2018;7(4):1285-1296.
37. Wang Y, Liu T, Yang N, Xu S, Li X, Wang D. Hypoxia and macrophages promote glioblastoma invasion by the CCL4-CCR5 axis. *Oncol Rep*. 2016;36(6):3522-3528.
38. Kruger M, Pietsch J, Bauer J, et al. Growth of endothelial cells in space and in simulated microgravity - a comparison on the secretory level. *Cell Physiol Biochem*. 2019;52(5):1039-1060.
39. Mortazavi A, Williams BA, McCue K, Schaeffer L, Wold B. Mapping and quantifying mammalian transcriptomes by RNA-Seq. *Nat Methods*. 2008;5(7):621-628.
40. Frazee AC, Perteza G, Jaffe AE, Langmead B, Salzberg SL, Leek JT. Ballgown bridges the gap between transcriptome assembly and expression analysis. *Nat Biotechnol*. 2015;33(3):243-246.
41. Bauer M, Goldstein M, Christmann M, Becker H, Heylmann D, Kaina B. Human monocytes are severely impaired in base and DNA double-strand break repair that renders them vulnerable to oxidative stress. *Proc Natl Acad Sci USA*. 2011;108(52):21105-21110.
42. Wunderlich R, Ernst A, Rodel F, et al. Low and moderate doses of ionizing radiation up to 2 Gy modulate transmigration and chemotaxis of activated macrophages, provoke an anti-inflammatory cytokine milieu, but do not impact upon viability and phagocytic function. *Clin Exp Immunol*. 2015;179(1):50-61.
43. Secchiero P, Rimondi E, di Iasio MG, Voltan R, Gonelli A, Zauli G. Activation of the p53 pathway induces α -smooth muscle actin expression in both myeloid leukemic cells and normal macrophages. *J Cell Physiol*. 2012;227(5):1829-1837.
44. Kim S, You D, Jeong Y, et al. TP53 upregulates α -smooth muscle actin expression in tamoxifen-resistant breast cancer cells. *Oncol Rep*. 2019;41(2):1075-1082.
45. Lee SY, Shin SJ, Kim HS. ERK1/2 activation mediated by the nutlin3-induced mitochondrial translocation of p53. *Int J Oncol*. 2013;42(3):1027-1035.
46. Lee SY, Choi HC, Choe YJ, Shin SJ, Lee SH, Kim HS. Nutlin-3 induces BCL2A1 expression by activating ELK1 through the mitochondrial p53-ROS-ERK1/2 pathway. *Int J Oncol*. 2014;45(2):675-682.
47. Biffi G, Oni TE, Spielman B, et al. IL1-induced JAK/STAT signaling is antagonized by TGFbeta to shape CAF heterogeneity in pancreatic ductal adenocarcinoma. *Cancer Discov*. 2019;9(2):282-301.
48. Ohlund D, Handly-Santana A, Biffi G, et al. Distinct populations of inflammatory fibroblasts and myofibroblasts in pancreatic cancer. *J Exp Med*. 2017;214(3):579-596.
49. Wang YY, Jiang H, Pan J, et al. Macrophage-to-myofibroblast transition contributes to interstitial fibrosis in chronic renal allograft injury. *J Am Soc Nephrol*. 2017;28(7):2053-2067.

50. Arderiu G, Espinosa S, Peña E, et al. Tissue factor variants induce monocyte transformation and transdifferentiation into endothelial cell-like cells. *J Thromb Haemost*. 2017;15(8):1689-1703.
51. Bellon A, Wegener A, Lescallete AR, et al. Transdifferentiation of human circulating monocytes into neuronal-like cells in 20 days and without reprogramming. *Front Mol Neurosci*. 2018;11:323.
52. Ludin A, Itkin T, Gur-Cohen S, et al. Monocytes-macrophages that express alpha-smooth muscle actin preserve primitive hematopoietic cells in the bone marrow. *Nat Immunol*. 2012;13(11):1072-1082.
53. Ye H, Zhou Q, Zheng S, et al. Tumor-associated macrophages promote progression and the Warburg effect via CCL18/NF-kB/VCAM-1 pathway in pancreatic ductal adenocarcinoma. *Cell Death Dis*. 2018;9(5):453.
54. Zhu Y, Herndon JM, Sojka DK, et al. Tissue-resident macrophages in pancreatic ductal adenocarcinoma originate from embryonic hematopoiesis and promote tumor progression. *Immunity*. 2017;47(2):323-338.e6.
55. Versteijne E, Vogel JA, Besselink MG, et al. Meta-analysis comparing upfront surgery with neoadjuvant treatment in patients with resectable or borderline resectable pancreatic cancer. *Br J Surg*. 2018;105(8):946-958.
56. Agarwal M, Biswas P, Bhattacharya A, Kumar Sinha D. ROS mediated cytoplasmic stiffening impairs the phagocytic ability of the macrophage. *J Cell Sci*. 2020;133(5):jcs236471.
57. Park EJ, Choi KS, Yoo YH, Kwon TK. Nutlin-3, a small-molecule MDM2 inhibitor, sensitizes Caki cells to TRAIL-induced apoptosis through p53-mediated PUMA upregulation and ROS-mediated DR5 upregulation. *Anticancer Drugs*. 2013;24(3):260-269.
58. Lowe JM, Menendez D, Bushel PR, et al. p53 and NF-kappaB coregulate proinflammatory gene responses in human macrophages. *Cancer Res*. 2014;74(8):2182-2192.
59. Bahrami A, Khazaei M, Bagherieh F, et al. Targeting stroma in pancreatic cancer: promises and failures of targeted therapies. *J Cell Physiol*. 2017;232(11):2931-2937.
60. Mahajan UM, Langhoff E, Goni E, et al. Immune cell and stromal signature associated with progression-free survival of patients with resected pancreatic ductal adenocarcinoma. *Gastroenterology*. 2018;155(5):1625-1639.e2.
61. Erkan M, Michalski CW, Rieder S, et al. The activated stroma index is a novel and independent prognostic marker in pancreatic ductal adenocarcinoma. *Clin Gastroenterol Hepatol*. 2008;6(10):1155-1161.
62. Elyada E, Bolisetty M, Laise P, et al. Cross-species single-cell analysis of pancreatic ductal adenocarcinoma reveals antigen-presenting cancer-associated fibroblasts. *Cancer Discov*. 2019;9(8):1102-1123.
63. Su S, Chen J, Yao H, et al. CD10(+)/GPR77(+) cancer-associated fibroblasts promote cancer formation and chemoresistance by sustaining cancer stemness. *Cell*. 2018;172(4):841-856.e16.
64. Ikenaga N, Ohuchida K, Mizumoto K, et al. CD10+ pancreatic stellate cells enhance the progression of pancreatic cancer. *Gastroenterology*. 2010;139(3):1041-1051, 1051.e1-8.

SUPPORTING INFORMATION

Additional supporting information may be found online in the Supporting Information section at the end of the article.

How to cite this article: Huang X, He C, Hua X, et al. Oxidative stress induces monocyte-to-myofibroblast transdifferentiation through p38 in pancreatic ductal adenocarcinoma. *Clin Transl Med*. 2020;10:e41.
<https://doi.org/10.1002/ctm2.41>